

Stability analysis for solving the 3D unsteady free-surface condition with raised panels

Tim H.J. Bunnik and Aad J. Hermans

Department of Applied Mathematics, Delft University of Technology, The Netherlands

1 Introduction

When the wave pattern around a sailing ship is predicted with an integral equation formulation, the amplitudes and lengths of these waves contain errors because the integral equation and boundary conditions must be discretized in order to solve it numerically. Of course we want these errors to be as small as possible, but we also want the computational effort to be as small as possible. We have therefore investigated how these errors depend on the discretization of the integral equation and the free-surface boundary condition with a stability analysis.

Recently, other people have also investigated the stability or accuracy of their numerical schemes. We combine the work of Raven [3], who analysed the accuracy of his numerical scheme for solving the steady problem, and Sierevogel [2], who analysed the stability of her numerical scheme for solving the unsteady problem. Both restricted their analysis to the two-dimensional case. We extend the analysis of Sierevogel to three dimensions and include the opportunity to use a raised panel surface like Raven did.

2 The time-domain algorithm

We consider a ship sailing at a constant high speed U in waves with an encounter frequency ω . We assume that the hydrodynamics can be described by potential flow and linear boundary conditions on the free surface and the hull of the ship. In [1] we show how the boundary conditions can be linearized about the flow and wave pattern caused by a steady moving ship in calm water. Far away from the ship, this flow can be approximated by a uniform flow. The boundary condition on the free surface then becomes

$$\frac{\partial^2 \phi}{\partial t^2} + 2U \frac{\partial^2 \phi}{\partial t \partial x} + U^2 \frac{\partial^2 \phi}{\partial x^2} + g \frac{\partial \phi}{\partial z} = 0 \quad \text{on } z = 0 \quad (1)$$

Because of simplicity we will use this condition, and not the complicated condition that we actually use, to analyse the accuracy and stability of our time-domain algorithm. The unknown potential is found by putting sources on the hull of the ship, Ω_2 , and on a surface, Ω_1 , at a short distance z_{fs} above the free surface. This raised surface has some advantages as we shall see. The potential is found to be

$$\phi(\vec{x}, t) = \iiint_{\Omega_1} \sigma(\vec{\xi}, t) G(\vec{x}, \vec{\xi}) d\vec{\xi} + \iiint_{\Omega_2} \sigma(\vec{\xi}, t) G(\vec{x}, \vec{\xi}) d\vec{\xi} \quad G = \frac{-1}{4\pi r} \quad (2)$$

If this expression is substituted in the boundary condition (1), a boundary integral equation for the source strength σ on the raised surface is found

$$W_1 \sigma = RHS \quad (3)$$

Integrals over the hull of the ship are shifted into a Right Hand Side, because in this abstract we only look at errors caused by discretizing the free surface. The raised surface is now divided into panels and on each panel the source strength is assumed to be constant. The integral (2) now turns into a summation over all panels of source strength times the integrated Green function. If we also

introduce difference schemes for the time derivatives and tangential space derivatives, we can solve the potential and corresponding wave pattern numerically. Because we solve discretized equations, the waves are different from the waves that would follow from the continuous equations (1) and (2). We will investigate the difference in wave length and wave amplitude by studying the linear operator W_1 in Fourier space.

3 The continuous case

The Fourier transform of the continuous free surface condition (1) and the continuous integral equation (2) can be obtained with the following pair of transforms

$$\tilde{\phi}(k, \theta, \omega) = \int_{-\infty}^{\infty} \int_{-\infty}^{\infty} \int_{-\infty}^{\infty} \phi(x, y, t) e^{-i(\omega t - kx \cos \theta - ky \sin \theta)} dx dy dt \quad (4)$$

$$\phi(x, y, t) = \frac{1}{(2\pi)^3} \int_{-\infty}^{\infty} \int_{-\pi}^{\pi} \int_0^{\infty} \tilde{\phi}(k, \theta, \omega) e^{i(\omega t - kx \cos \theta - ky \sin \theta)} k dk d\theta d\omega \quad (5)$$

k is the wave number; θ the wave angle and ω the wave frequency. After some calculations it can be shown that the Fourier transform of the linear operator W_1 equals

$$\tilde{W}_1 = \tilde{G}(-\omega^2 + 2Uk\omega \cos \theta - U^2k^2 \cos^2 \theta + gk) \quad (6)$$

After transforming back, the potential turns out to be

$$\phi(x, y, t) = \frac{1}{(2\pi)^3} \int_{-\infty}^{\infty} \int_{-\pi}^{\pi} \int_0^{\infty} \frac{RHS \tilde{G}}{\tilde{W}_1} e^{i(\omega t - kx \cos \theta - ky \sin \theta)} k dk d\theta d\omega \quad (7)$$

The zeros of the operator \tilde{W}_1 give the wave-like contributions of this integral. The dispersion relation $\tilde{W}_1(k, \theta, \omega) = 0$ therefore has to be solved. It can be shown that the behaviour of the solution depends on the Strouhal number $\tau = \frac{\omega U}{g}$. We will restrict our analysis to speeds and frequencies for which $\tau > \frac{1}{4}$. This can be done because we assume the speed of the ship, and therefore also the encounter frequencies of the incoming waves, to be high. When $\tau > \frac{1}{4}$, the solutions of the dispersion relation are

$$k_{\pm} = \begin{cases} \frac{g}{4U^2 \cos^2 \theta} (1 \pm \sqrt{1 + 4\tau \cos \theta})^2 & \text{if } 1 + 4\tau \cos \theta \geq 0, \\ \frac{g}{4U^2 \cos^2 \theta} (1 \pm i\sqrt{-1 - 4\tau \cos \theta})^2 & \text{if } 1 + 4\tau \cos \theta < 0 \end{cases} \quad (8)$$

So, if $1 + 4\tau \cos \theta < 0$, the wave number has a non-zero imaginary part, which means that these waves disappear rapidly when they propagate up- or downstream. If $1 + 4\tau \cos \theta \geq 0$, the integration contour in (7) can be chosen such, that the solution only contains waves that propagate downstream, see for example [4]. We therefore only concentrate on downstream wave angles i.e. $-\frac{\pi}{2} \leq \theta \leq \frac{\pi}{2}$.

4 The discrete case

We now discretize the raised surface and the time and space derivatives in the free surface condition (1). The raised surface is divided into rectangular panels of size $\Delta x \times \Delta y$. The height of this raised surface above the free surface $z = 0$ is proportional to the area of these panels according to $z_{fs} = \alpha \sqrt{\Delta x \Delta y}$. The potential can now be written as an infinite sum over all panels:

$$\phi(x_m, y_n) = \sum_{i=-\infty}^{\infty} \sum_{j=-\infty}^{\infty} \sigma_{ij} \int_{(i-\frac{1}{2})\Delta x}^{(i+\frac{1}{2})\Delta x} \int_{(j-\frac{1}{2})\Delta y}^{(j+\frac{1}{2})\Delta y} \frac{-dx_0 dy_0}{4\pi \sqrt{(x_m - x_0)^2 + (y_n - y_0)^2 + z_{fs}^2}} \quad (9)$$

The collocation points (x_m, y_n) lie on the free surface at a vertical distance z_{fs} from the middle of a panel, so $x_m = m\Delta x$ and $y_n = n\Delta y$.

The derivatives can be discretized as follows:

$$\frac{\partial^2 \phi}{\partial t^2}(t_{i+1}) = \frac{1}{(\Delta t)^2} \left(d_0^{(tt)} \phi(t_{i+1}) + d_{-1}^{(tt)} \phi(t_i) + d_{-2}^{(tt)} \phi(t_{i-1}) + d_{-3}^{(tt)} \phi(t_{i-2}) \right) \quad (10)$$

$$\frac{\partial^2 \phi}{\partial x^2}(x_{i+1}) = \frac{1}{(\Delta x)^2} \left(d_0^{(xx)} \phi(x_{i+1}) + d_{-1}^{(xx)} \phi(x_i) + d_{-2}^{(xx)} \phi(x_{i-1}) + d_{-3}^{(xx)} \phi(x_{i-2}) \right) \quad (11)$$

Similar formulae apply to the first order derivatives $\frac{\partial \phi}{\partial t}$ and $\frac{\partial \phi}{\partial x}$. The coefficients $d^{(tt)}$, $d^{(xx)}$, $d^{(x)}$ and $d^{(t)}$ can be chosen such that a first or second order difference scheme is obtained. We use upwind differences for the space derivatives, which means that only points upstream from the collocation point in question are used in the difference scheme. We do this, because it is the only way to obtain a stable scheme for high speeds as shown in [2]. We now use the discrete Fourier transform to obtain the wave number in the discretized case. This transform and its inverse are defined by

$$\hat{\phi}(k, \theta, \omega) = \Delta x \Delta y \Delta t \sum_{m=-\infty}^{\infty} \sum_{n=-\infty}^{\infty} \sum_{p=-\infty}^{\infty} \phi(x_m, y_n, t_p) e^{-i(\omega p \Delta t - km \Delta x \cos \theta - kn \Delta y \sin \theta)} \quad (12)$$

$$\phi(x_m, y_n, t_p) = \frac{1}{(2\pi)^3} \int_{-\frac{\pi}{\Delta t}}^{\frac{\pi}{\Delta t}} \int_{-\frac{\pi}{\Delta y}}^{\frac{\pi}{\Delta y}} \int_{-\frac{\pi}{\Delta x}}^{\frac{\pi}{\Delta x}} \hat{\phi}(k, \theta, \omega) e^{i(\omega p \Delta t - km \Delta x \cos \theta - kn \Delta y \sin \theta)} d(k \cos \theta) d(k \sin \theta) d\omega \quad (13)$$

If we apply this transform to the discretized boundary condition and integral equation, we find the discrete Fourier transform of the operator \hat{W}_1 .

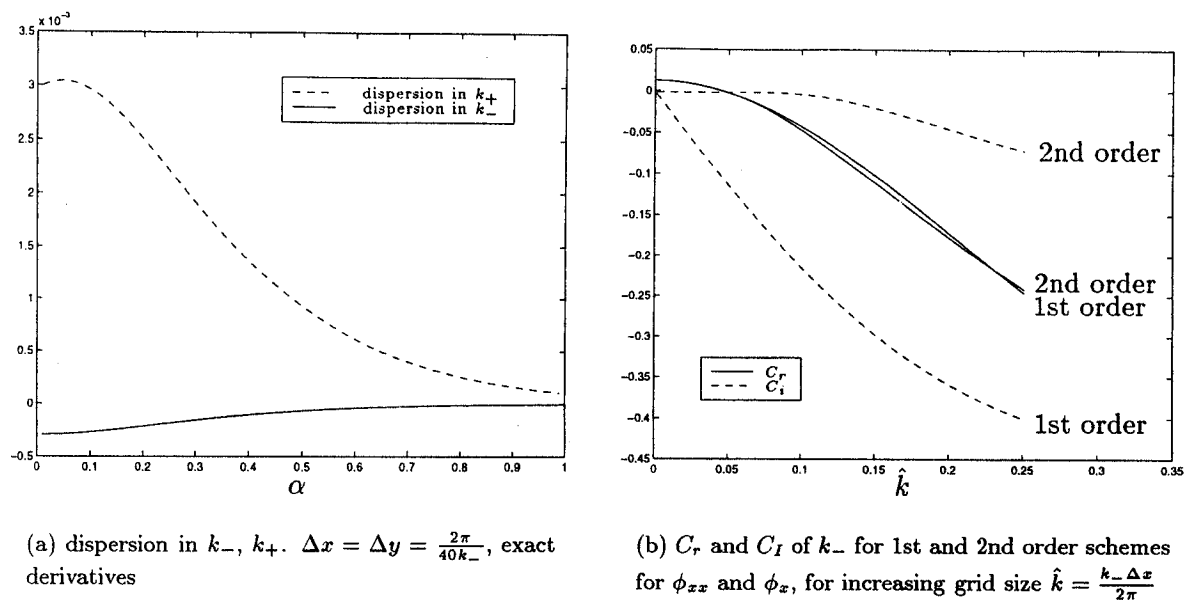
$$\begin{aligned} \hat{W}_1 = & \frac{\hat{G}}{\Delta x \Delta y} \left(\frac{1}{(\Delta t)^2} \left(d_0^{(tt)} + d_{-1}^{(tt)} e^{-i\omega \Delta t} + d_{-2}^{(tt)} e^{-2i\omega \Delta t} + d_{-3}^{(tt)} e^{-3i\omega \Delta t} \right) + \right. \\ & \frac{2U}{\Delta x \Delta t} \left(d_0^{(x)} + d_{-1}^{(x)} e^{ik \Delta x \cos \theta} + d_{-2}^{(x)} e^{2ik \Delta x \cos \theta} \right) \left(d_0^{(t)} + d_{-1}^{(t)} e^{-i\omega \Delta t} + d_{-2}^{(t)} e^{-2i\omega \Delta t} \right) + \\ & \left. \frac{U^2}{(\Delta x)^2} \left(d_0^{(xx)} + d_{-1}^{(xx)} e^{ik \Delta x \cos \theta} + d_{-2}^{(xx)} e^{2ik \Delta x \cos \theta} + d_{-3}^{(xx)} e^{3ik \Delta x \cos \theta} \right) + g \frac{\hat{Q}}{\hat{G}} \right) \quad (14) \end{aligned}$$

\hat{G} is the discrete Fourier transform of the integrated green function, and \hat{Q} the discrete Fourier transform of the integrated vertical derivative of the Green function, $\frac{\partial G}{\partial z}$. After some complicated manipulations it can be shown that these transforms equal

$$\hat{G} = \sum_{m=-\infty}^{\infty} \sum_{n=-\infty}^{\infty} \frac{e^{-z_{fs} \sqrt{\alpha_m^2 + \beta_m^2}}}{2\alpha_m \beta_m \sqrt{\alpha_m^2 + \beta_m^2}} \left(e^{-\frac{1}{2}i\Delta x \alpha_m} - e^{\frac{1}{2}i\Delta x \alpha_m} \right) \left(e^{-\frac{1}{2}i\Delta y \beta_n} - e^{\frac{1}{2}i\Delta y \beta_n} \right) \quad (15)$$

$$\hat{Q} = \sum_{m=-\infty}^{\infty} \sum_{n=-\infty}^{\infty} \frac{e^{-z_{fs} \sqrt{\alpha_m^2 + \beta_m^2}}}{2\alpha_m \beta_m} \left(e^{-\frac{1}{2}i\Delta x \alpha_m} - e^{\frac{1}{2}i\Delta x \alpha_m} \right) \left(e^{-\frac{1}{2}i\Delta y \beta_n} - e^{\frac{1}{2}i\Delta y \beta_n} \right) \quad (16)$$

where $\alpha_m = k \cos \theta + \frac{2\pi m}{\Delta x}$ and $\beta_n = k \sin \theta + \frac{2\pi n}{\Delta y}$. Only a small number of terms has to be taken into account because these series converge very fast. The zeros of the discrete operator \hat{W}_1 correspond with the discrete wave numbers and can be found numerically. They can be compared with the continuous ones and any differences indicate errors.

Figure 1: Results for $U = 1.25$, $\omega = 20$, $\theta = 0$

5 Damping, dispersion and temporal stability

We can relate the continuous wave number k_c and the discrete wave number k_d by writing

$$k_d = k_c (1 + C_R(\omega, U, \theta, \Delta t, \Delta x, \Delta y, \alpha) + iC_I(\omega, U, \theta, \Delta t, \Delta x, \Delta y, \alpha)) \quad (17)$$

Non-zero C_r or C_I indicate an error in the discrete wave number. If C_R is negative, this means the wave number is too small, so the predicted wave length is too large. A positive C_R indicates an under estimation of the wave length. A positive C_I indicates numerical amplification, and a negative C_I numerical damping. We have investigated the dependence of these errors on the difference schemes, the time step, the grid size and the distance from panels to free surface for various speeds, frequencies and wave angles. It turned out that the use of second order difference schemes for the space derivatives reduces damping drastically compared to the use of first order difference schemes, as can be seen in figure 1(b). Furthermore, it was found that the use of raised panels reduces numerical dispersion. As can be seen in figure 1(a), the dispersion decreases if the distance from panels to free surface is increased. If this distance becomes too large, the time integration is not temporal stable anymore. This temporal stability can be investigated by rewriting the dispersion relation. If we substitute $Z = e^{-i\omega\Delta t}$, we obtain a third order complex relation for Z , which has three roots. If one or more of these roots is outside the unit circle in the complex plane, the numerical scheme is temporal unstable.

References

- [1] T.H.J. Bunnik *Motions of a vessel at high speed*. Report 97-11, Delft University of technology.
- [2] L.M. Sierevogel *Time-Domain Calculations of Ship Motions*. PhD Thesis, Delft University of Technology, 1998.
- [3] H.C. Raven. *A Solution Method for the Nonlinear Ship Wave Resistance Problem*. PhD Thesis, Delft University of Technology, 1996.
- [4] J.V. Wehausen and E.V. Laitone. *Surface waves*, volume 9 of *Encyclopedia of physics*. Springer-Verlag, Berlin, Germany, 1960.